Journal of Magnetism and Magnetic Materials 643 (2026) 173915

Contents lists available at ScienceDirect

Journal of Magnetism and Magnetic Materials

journal homepage: www.elsevier.com/locate/jmmm

Design concepts of end poles and measurements of an asymmetric magnet pole undulator

Rohit Kamle [a], G. Mishra [a,*], Roma Khullar [b], Mona Gehlot [c], Saif Mohd Khan [d]

[a] School of Physics, Devi Ahilya VishwaVidyalaya, Indore 452001, India
[b] Government Holkar Science College, Indore 452001, India
[c] Deutsches Elektronen-Synchrotron DESY, Hamburg, Germany
[d] Synchrotron SOLEIL, Saint Aubin 91190, France

ARTICLE INFO

Keywords:
Undulator
Asymmetric magnet pole undulator

ABSTRACT

The Design concepts of an asymmetric magnet pole undulator-prototype is presented. The asymmetric magnet pole undulator is designed with upper and the lower magnet arrays of 25 mm and 50 mm period lengths respectively. Novel features of the magnetic measurements of the magnet arrays are presented and analyzed with an alternate tunable end-termination scheme. The lower 50 *mm* period array employs a vertically magnetized end half magnet with a provision of 3.125 *mm* longitudinal movement. The end magnet of the upper magnet array with 25 *mm* period length has a scope of vertical movement of 3.125 mm. We propose to minimize the field integral by longitudinal and vertical movements of the end half magnets.

1. Introduction

In recent years there are interests on undulator technology with design and development of new generation high quality undulator for synchrotron radiation light sources and free electron lasers. The undulator is a periodic arrangement of dipole magnets designed in Halbach arrangement to provide a sinusoidal magnetic field to the relativistic electron beam. The relativistic electron beam while propagating over the undulator length emits electromagnetic wave and is the basis of development of synchrotron radiation source and free electron laser facilities. In its standard Halbach field configuration, the undulator is designed with a uniform gap where an upper and lower magnet array constitutes the undulator. Both the upper and lower magnet arrays have the same period lengths. Four dipole magnets make one undulator period. The undulator length consists of several number of periods. The undulator axis is the geometric axis of the gap between the magnet arrays. The APPLE undulator [1,2], the Knot undulator [3],the APPLE-Knot undulator [3], the biperiod undulator [4], the double period undulator [5], the asymmetric magnet pole undulator [6],the Delta undulator [7],the transverse gradient undulator [8,9],the quasi periodic undulator [10,11] are examples of some of the Genext undulators that have seen renewed interests for technology upgradation in synchrotron radiation sources and free electron lasers. The end termination of the undulator is the key to performance of the undulator. Mostly the end section of the undulator is terminated by a half magnet [12–16]. However, novel undulators adopt novel end terminating schemes such as in biperiod undulators [17], the Delta undulator [18] and double undulators.

The asymmetric magnet pole undulator [19–23] has been reported for capable of producing circularly polarized light at off axis and can operate in quasi period mode to prevent higher harmonics in axis. In this paper, we present a tunable scheme of end terminating scheme for development of an asymmetric magnet pole undulator. The upper and the lower magnet arrays of the asymmetric magnet pole undulator will have different period lengths. As a consequence the asymmetric magnet pole undulator defines different magnet field profiles at different beam axis. In section II, we present the RADIA simulation studies of both the magnet arrays and report an alternate scheme of end field termination of the undulator. The end termination has an advantage of flexible tuning of the magnetic field integrals. In section III, we present mechanical structure of the magnet arrays. In section IV, we discuss the preliminary investigations of the field integrals and compare the results with RADIA. A conclusion and future ongoing activities are discussed in section V.

* Corresponding author.
E-mail address: gmishra_dauniv@yahoo.co.in (G. Mishra).

https://doi.org/10.1016/j.jmmm.2026.173915
Received 21 July 2025; Received in revised form 17 December 2025; Accepted 6 February 2026
Available online 12 February 2026

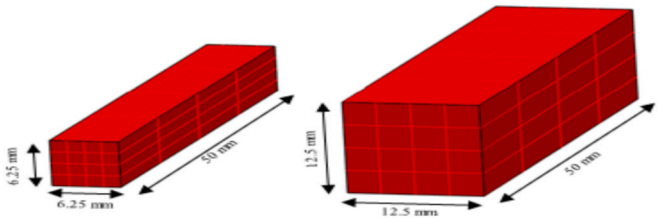

Fig. 1. Radia model of single magnets.

2. Radia simulation

The Radia [24,25] is a 3D magnetostatics computer code used for design and optimizing undulator for Synchrotron Light Sources and free electron lasers. In this paper, we propose to design an asymmetric magnet pole undulator. In the prototype undulator design, the upper magnet array period length as $\lambda_{u1} = 25mm$. The three-dimensional size of the magnet blocks is represented as W_x, W_y, W_z along x, y, $z$directions. The coordinates x, y represents the horizontal and vertical direction. The coordinate z is the longitudinal beam direction. The upper magnets have dimensions are $W_x = 50$mm, $W_y = 6.25$mm, $W_z = 6.25mm$ respectively. The NdFeB magnets are rectangular in cross section. The lower array has a period length of $\lambda_{u2} = 50mm$. The lower magnet blocks have $W_x = 50$mm, $W_y = 12.5$mm, $W_z = 12.5mm$ (Fig. 1). Four magnets will constitute a period of 50 mm period length.

Fig. 2a represents the standard end termination scheme with half-magnet for the lower 50 mm period length array. The magnetization is vertically upward and the size of the end magnet is $W_x = 50$mm, $W_y = 12.5$mmand $W_z = 6.25mm$. The volume of the full magnet is 50 mm × 12.5 mm × 12.5 mm is 7812.5 mm^3. The volume of the end magnet (50 mm × 12.5 mm × 6.25 mm) is 3906.25 mm^3. The volume ratio of the end magnet to the regular magnet is 1/2. In the schemes 2b, 2c and 2d the end magnet size is $W_x = 50$mm, $W_y = 6.25$ mmand $W_z = 12.5mm$. The magnetization is still vertically upward but the magnet is translated from downward to upward. In scheme 2d such as in Fig. 2d, the end magnet is located at the center of the regular magnet. In scheme 2b, the end magnet is located at the lower position and in scheme 2c, the magnet is located at the upper position.

In Fig. 3, we plot the magnetic field in RADIA for all the schemes. Fig. 4 plots the magnetic field and the first field integral with all these schemes. The scheme in Fig. 2a and d are equivalent schemes offering minimum field integral. The schemes 2b and c offers opposite values. Fig. 5 plots the second field integral. The schemes Fig. 2a and d compute the same second field integral from RADIA. There is additional information contained in Figs. 4 and 5. By translating the end magnet vertically upward and vertically downward, the field integrals are tuned.

Fig. 6 represents the end schemes of the 25 mm period length array. The scheme in Fig. 6a is the standard end magnet scheme. The volume of the regular magnet is 6.25 mm × 6.25 mm × 50 mm =1953.125 mm^3. The volume of the end magnet is 6.25 mm× 3.125 mm × 50 mm =976.5625 mm^3. The ratio of the volume of the end magnet to the regular magnet is 1/2. In Figs. 6b, c and d the magnet location is translated from upward to downward. In Fig. 6d, the magnet is located at the center of the regular magnet. Fig. 7 represents the magnetic field for all these schemes. Fig. 8 represents the first field integral. The plots yield the result that scheme 6a and scheme 6d are equivalent in geometry to provide minimum field integral.Fig. 9 illustrates the second field integral and supports the result obtained as in Fig. 8. The scheme 6d is equivalent to scheme 6a. However, scheme 6d provides additional feature that the field integral can be tuned by translating the magnet location vertically upward to downward.

In Fig. 10, the tunability of second field integral is shown. By

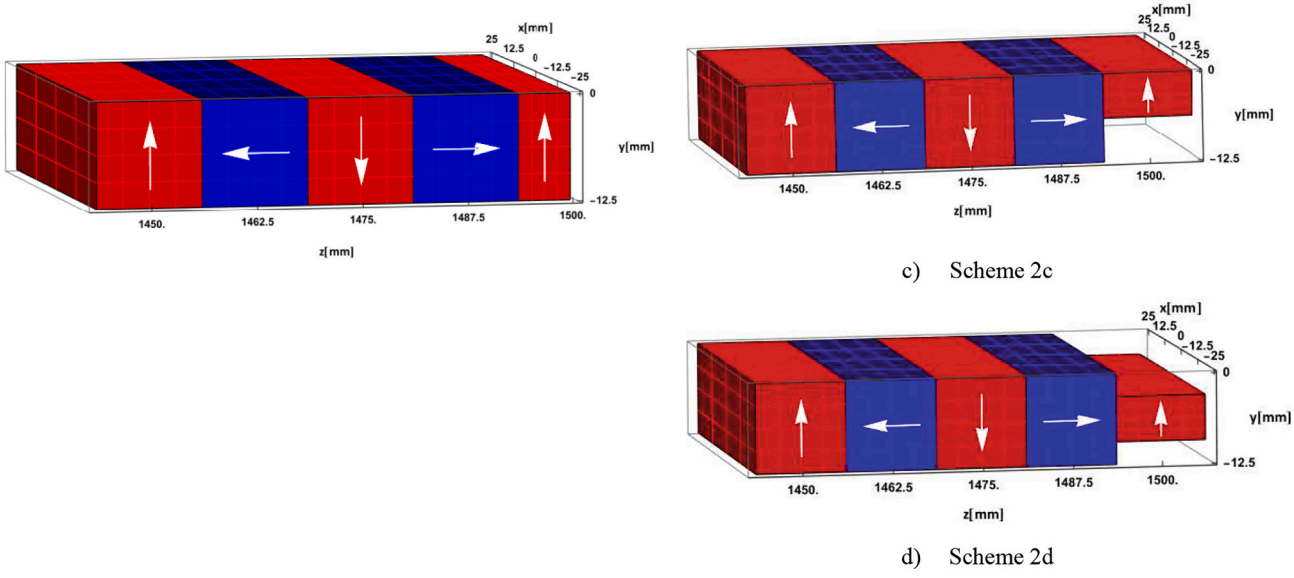

Fig. 2. Radia model of undulator end termination schemes.

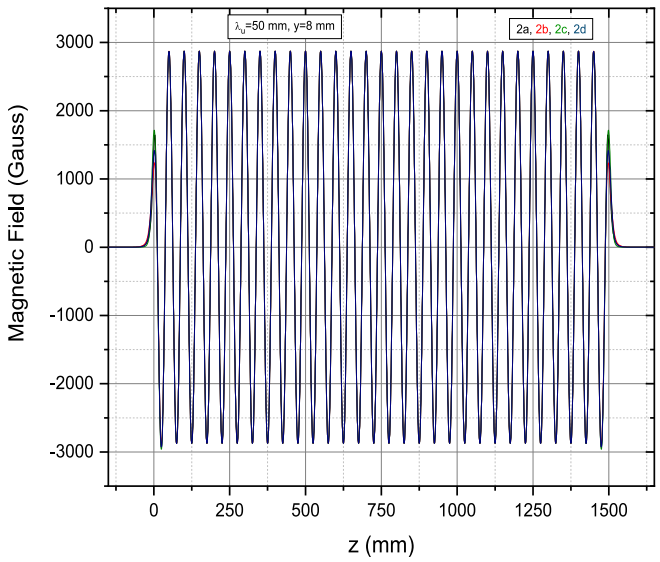

Fig. 3. Radia magnetic field for different schemes.

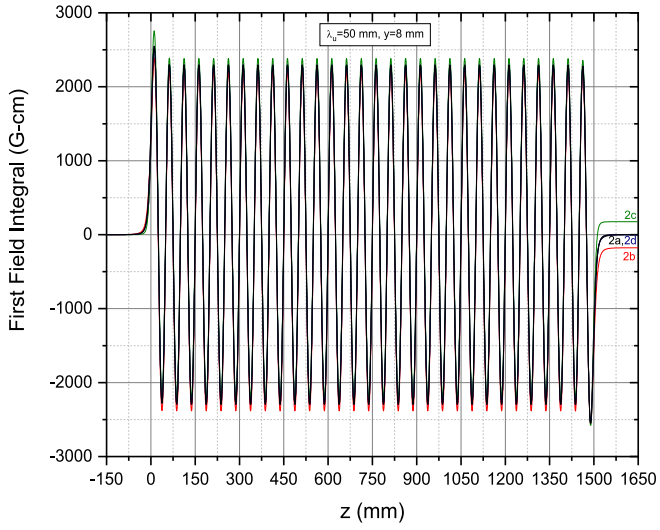

Fig. 4. Radia first field integral for different schemes.

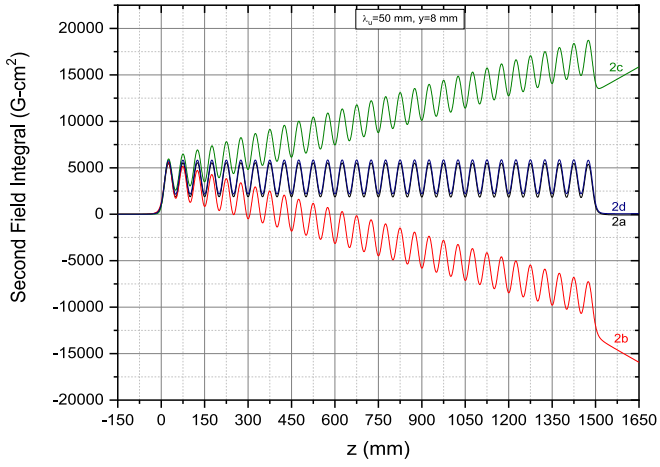

Fig. 5. Radia second field integral for different schemes – lower keeper.

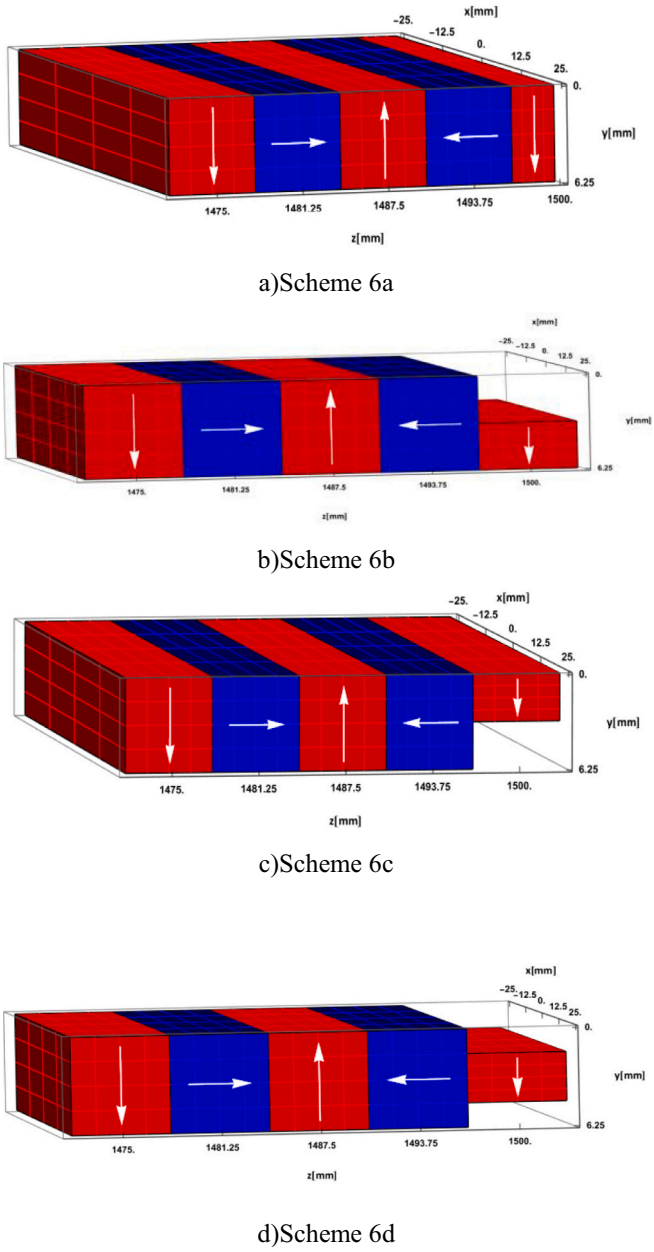

Fig. 6. Radia model of undulator end termination schemes.

vertically shifting the end magnet position from downward to upward in small steps, we can obtain a range of second field integral values, which is minimum for middle position. In the present design,the scheme 6d, for the 25 mm period length magnet array offers a tuning of 2000 Gcm^2 field integral value.

3. Mechanical design of the magnet arrays

The magnet keeper is 1525 mm in length (Fig. 11).It accommodates 60 periods, 25 mm each period length. An extra 25 mm is kept to account for the oversize of the magnets and to allow flexible end terminations. Fig. 11b represents the cross sectional view of the magnet keeper. The hole-to-hole distance is 68.25 mm. The magnet W_x length is 50 mm. A length of 18.25 mm at each end accounts for the place of the T clamps. The two clamp widths and the magnet length of 50 mm defines the grove length of 86.5 mm. The total groove width is 112 mm and height is 33.25 mm (Fig. 11c) The T clamps overhangs the magnets by 2 mm in height and 5 mm in length. Thus, a length (50 mm- 5 mm × 2) of

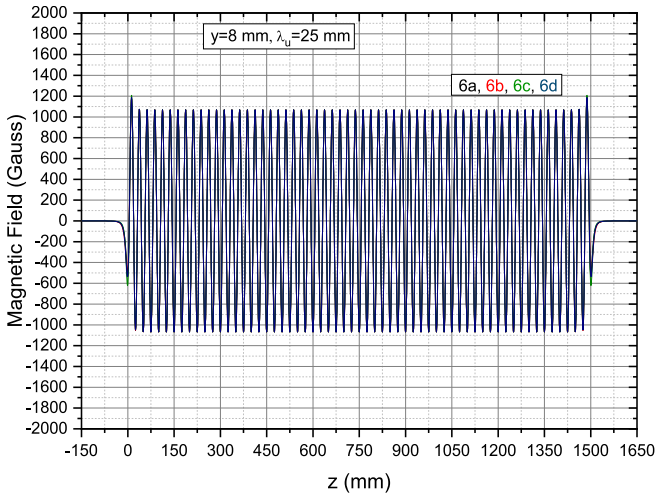

Fig. 7. Radia magnetic field for different schemes – upper keeper.

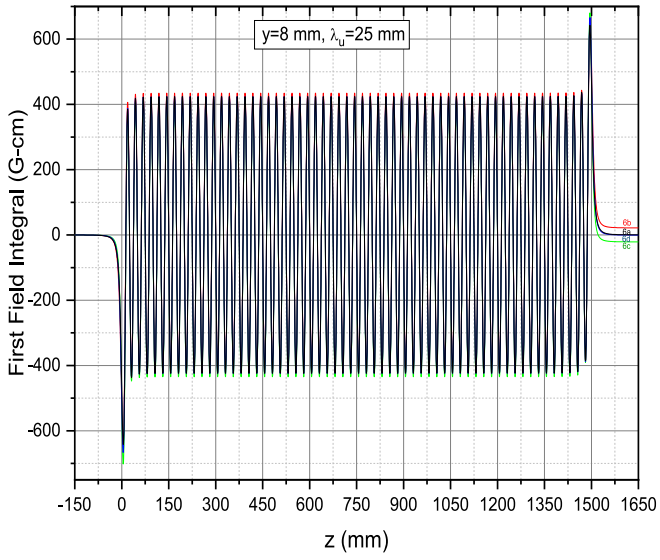

Fig. 8. Radia first field integral for different schemes – upper keeper.

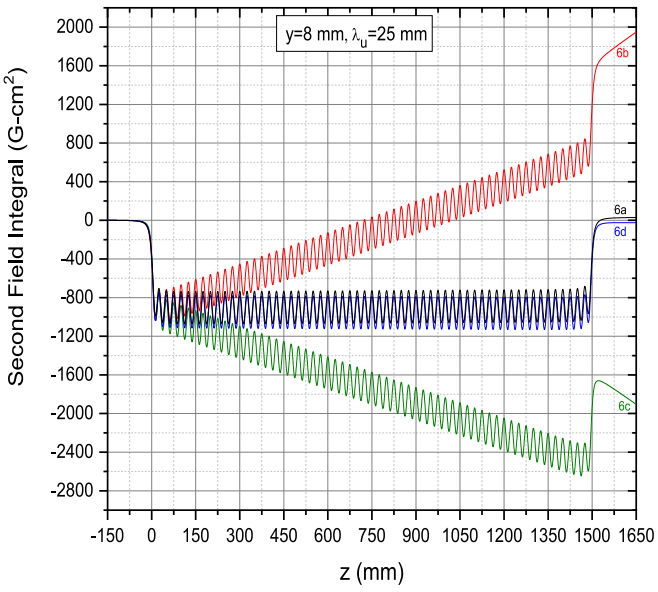

Fig. 9. Radia second field integral for different schemes – upper keeper.

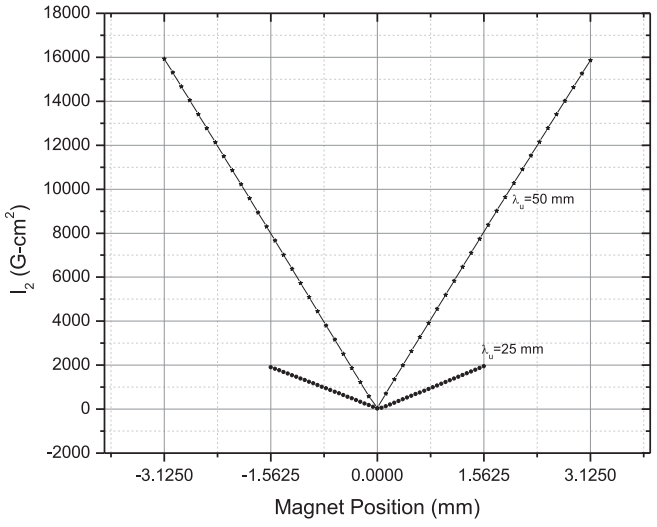

Fig. 10. Tuning of second field integral with the vertical movement of the end magnet.

40 mm is available for good field region measurements. Scheme 2a is used as the end termination of this magnet array.

There will be 30 periods which will be assembled in the 1500 mm keeper length. An extra length of 12.5 mm is kept at both the ends. It will take care of the oversize of the magnets and allow flexible end terminations. The end magnets of length 6.25 mm are used. Fig. 12a represents the lower magnet keeper. `. 12b and c represent the cross sectional view of the magnet keeper without and with the T clamps. Except the hole tapping all the dimensions are same as in the upper magnet keeper. Scheme 6d is used for the end termination.

4. Measurement & results

In the prototype asymmetric type magnet pole undulator design, we adopt the concepts of Figs. 2a and 6d as the end termination schemes. The motivation and objective to adopt scheme Fig. 6d is to introduce additional tuning to the field integral values. Fig. 13a, b and c give magnetic field, first field and second field integral of the lower magnet array with 50 mm period length. The 50 mm period magnet array has an end termination scheme as in Fig. 2a. There is a disagreement of first field integral value of 1000 G-cm from RADIA. The second field integral value of the designed magnet array provides a value of 40,000 Gcm2 higher than RADIA. Fig. 14a, b and c show the magnetic field, first and second field integrals for the upper magnet array with 25 mm period length. The end terminal scheme is scheme as in Fig. 6d for the keeper. The first integral value is 200 G-cm and the second field integral value is 14,000 G-cm^2 for the lower keeper. The angular offset and trajectory offset can be calculated from

$$\frac{0.3}{GeV} I_1(Tm) \text{ radian}$$

$$\frac{0.3}{GeV} I_2(Tm^2) \text{ meter}$$

This allows a trajectory correction of 0.3 mm with a 18 MeV electron beam with tunability second field integral value of 2000 G-cm^2. The good field region of the 50 mm array and 25 mm array are shown in Figs. 15 and 16 respectively at different vertical heights.

In Fig. 17, the magnetic field is plotted at different vertical heights from the two magnet arrays. The magnet axis will be defined as the axis

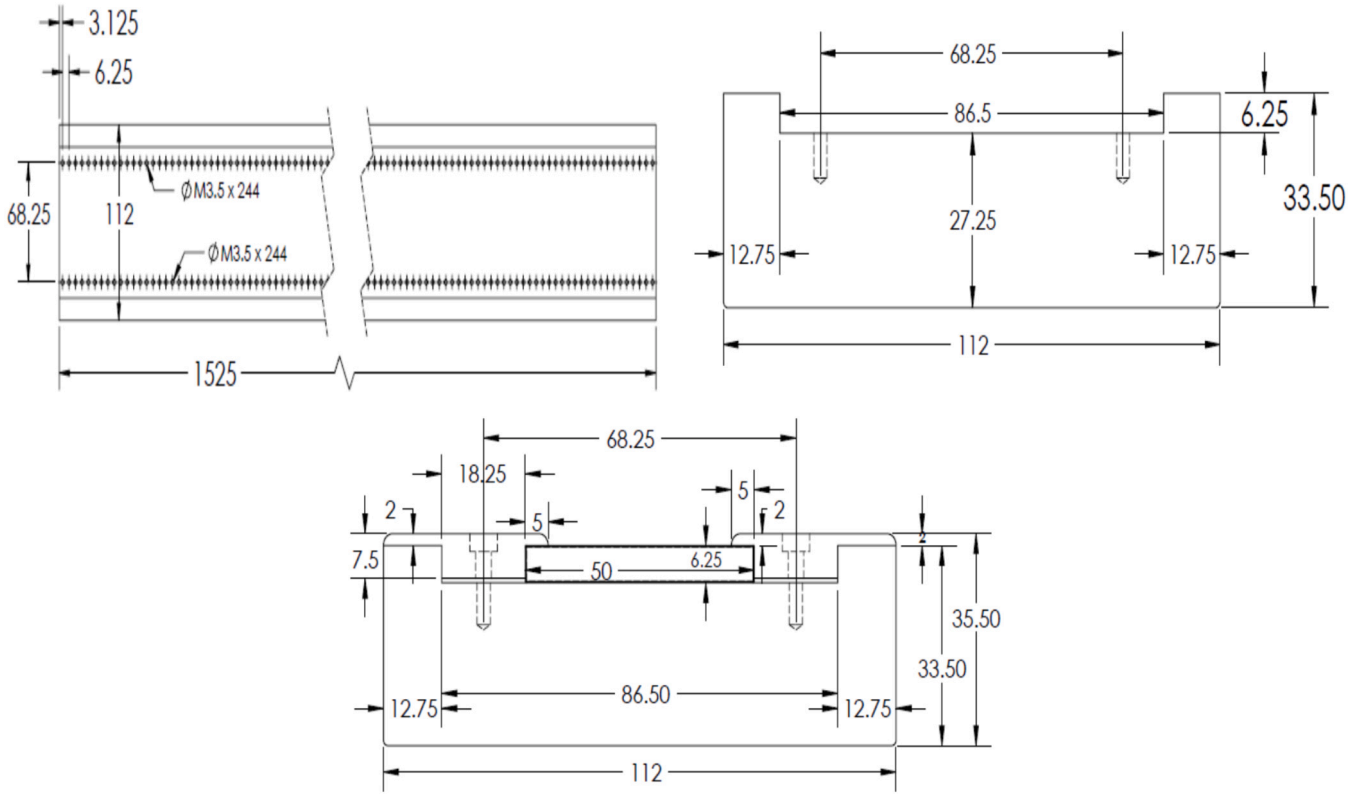

Fig. 11. 25 mm period upper magnet array. Cross sectional view of the 25 mm period upper magnet array. Cross sectional view of the 25 mm period magnet array with T clamps.

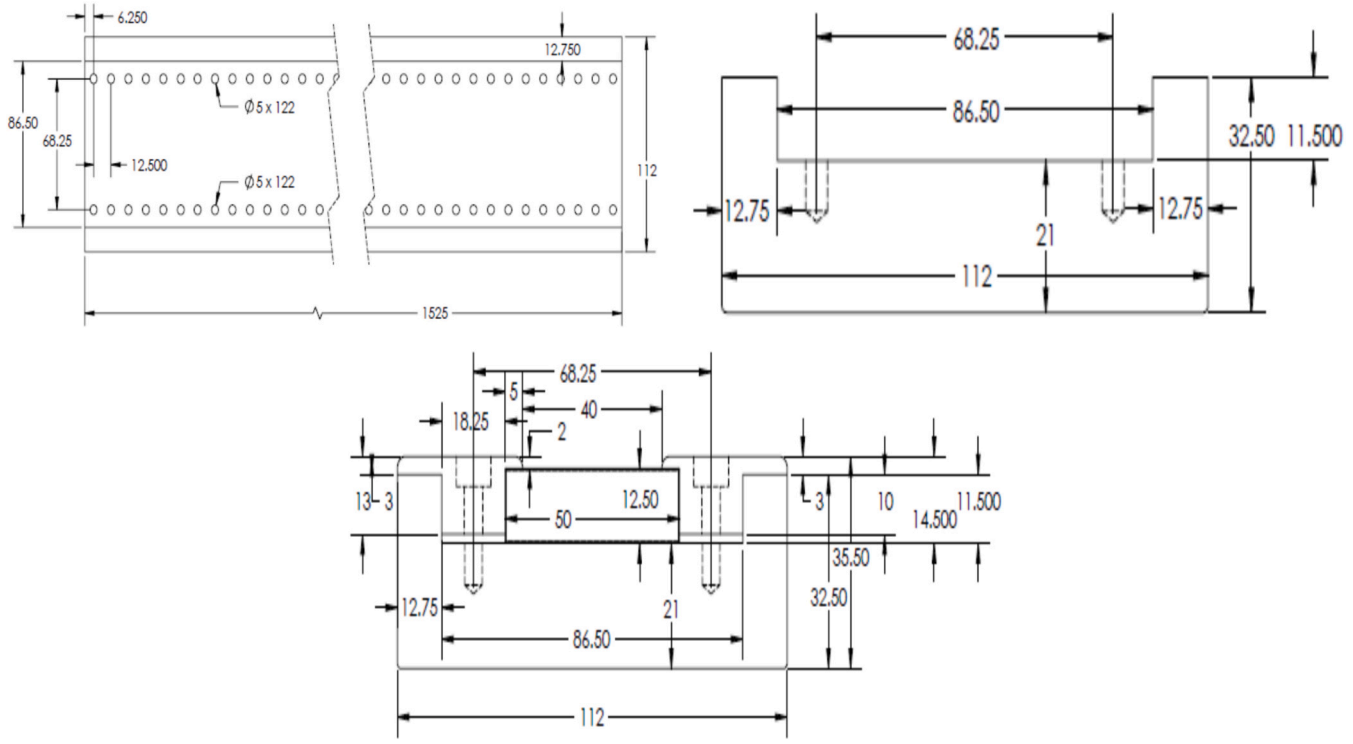

Fig. 12. 50 mm period lower magnet array. Cross sectional view of the 50 mm period magnet array.Cross sectional view of the 50 mm period magnet array with T clamps.

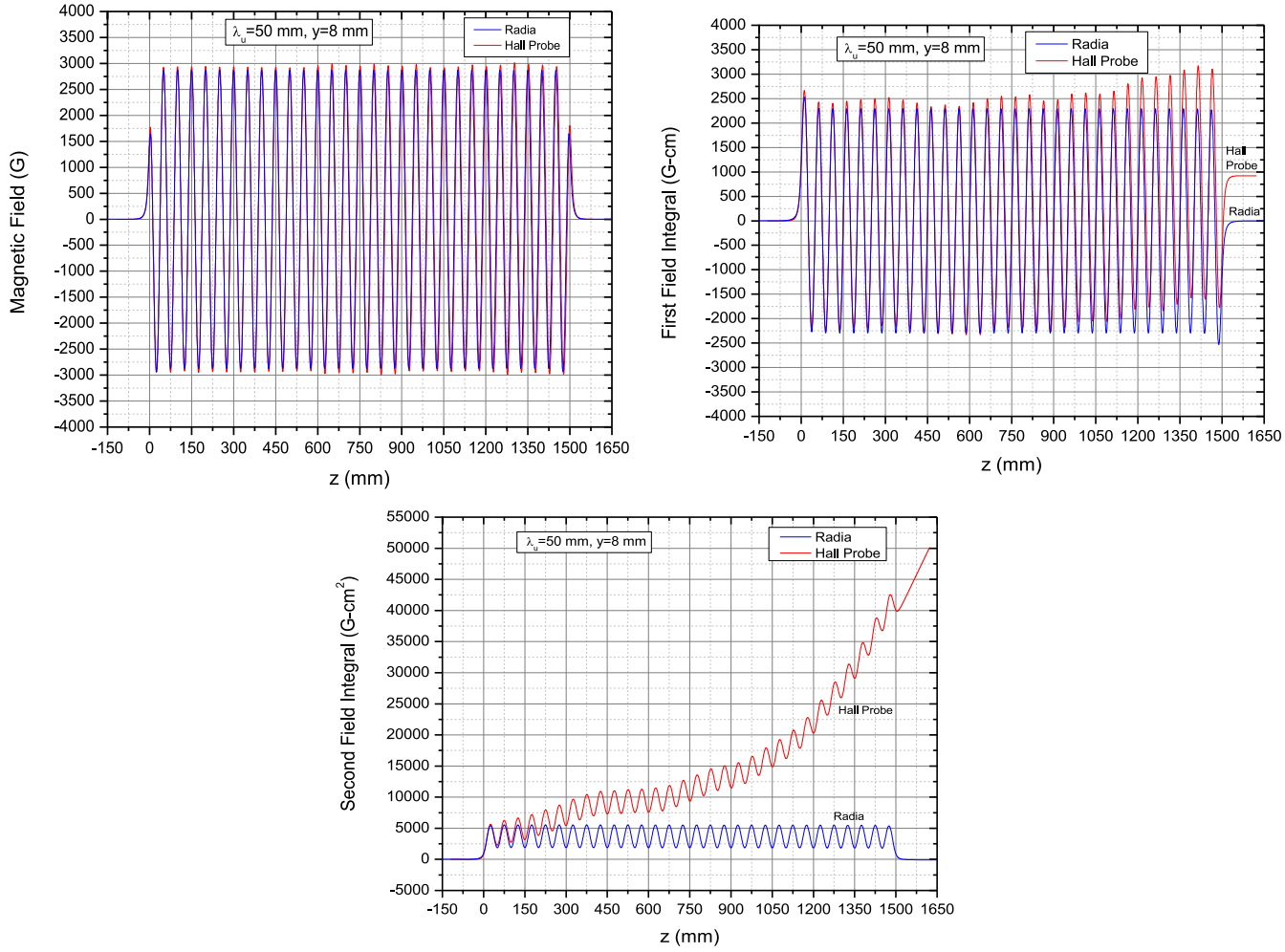

Fig. 13. Magnetic field in Hall Probe and Radia for scheme 2a. First field Integral Hall Probe and Radia for scheme 2a. Second field integral Hall Probe and Radia for scheme 2a.

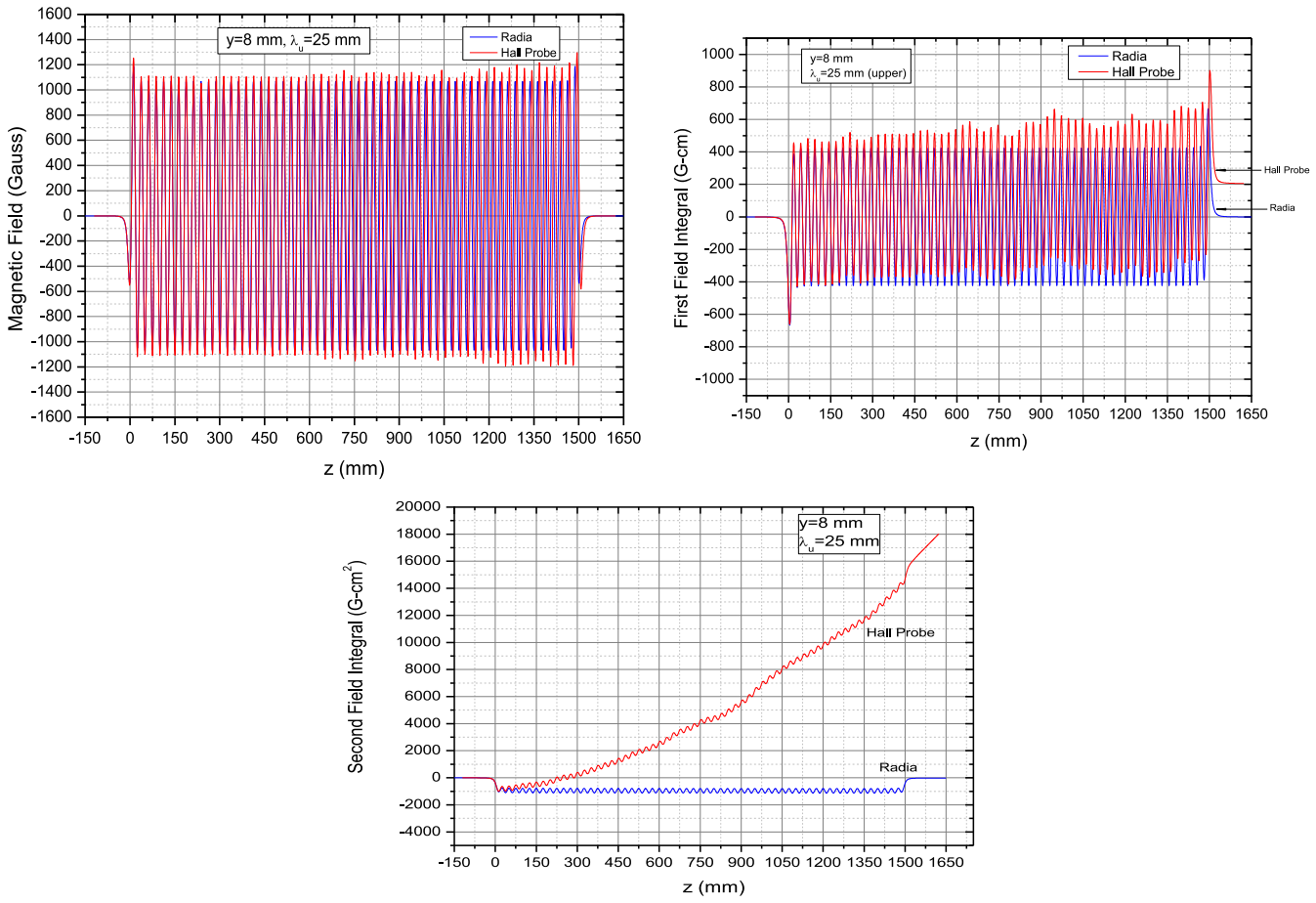

Fig. 14. Hall Probe and Radia magnetic field for scheme 6d for 25 mm period magnet array. Hall Probe and Radia first field integral for scheme 6d for the 25 mm period magnet array. Comparison of Hall Probe and Radia for scheme 6d - Second field integral for upper keeper.

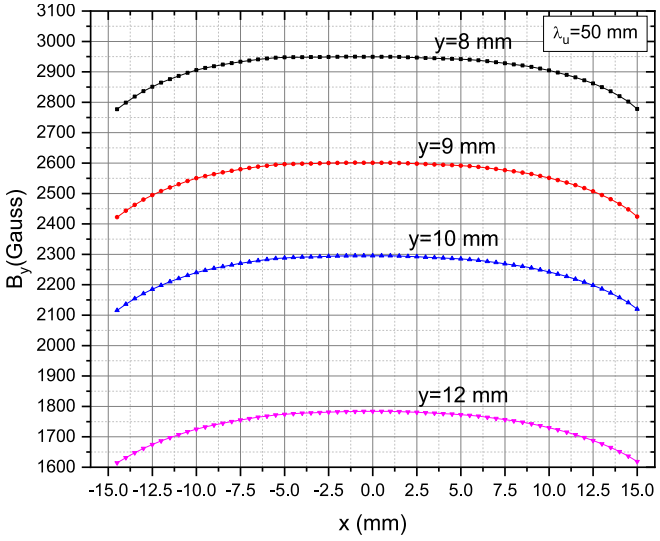

Fig. 15. Good field region for the 50 mm period magnet array.

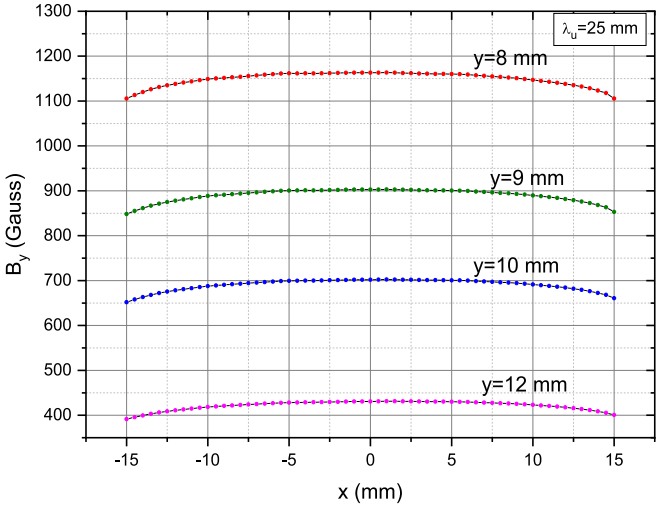

Fig. 16. Good field region for the 25 mm period magnet array.

where two magnet arrays produce the same magnetic field. The device will produce 2320 G at a gap of 23.5 mm gap. In Fig. 18, we plot the difference in peak values of magnetic field from the average magnetic field from Hall probe measurements (Figs. 13a and 14a). The deviation of the peak magnetic field from the average value is limited to 100 G.

5. Conclusion

The magnetic measurements of the magnet arrays of an asymmetric magnet pole undulator-prototype is presented. The conventional undulator has in general two end termination schemes [12]. The simplest method to ensure a zero first integral of the vertical magnetic field is to use a vertically magnetized half-length block at each end of the array. In

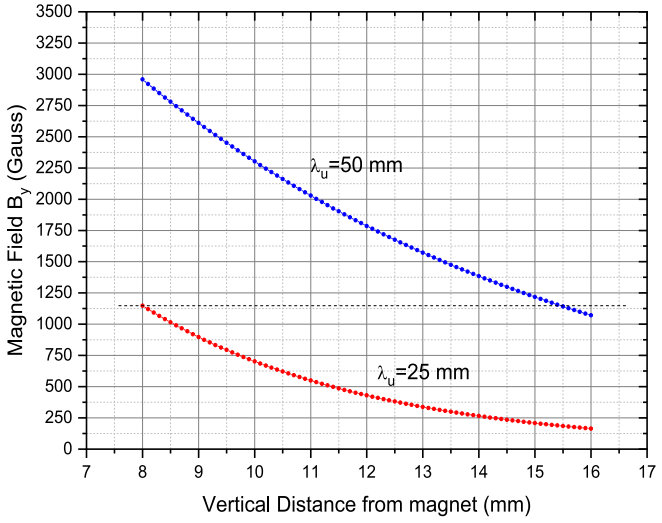

Fig. 17. Magnetic field with gap for both the magnet arrays.

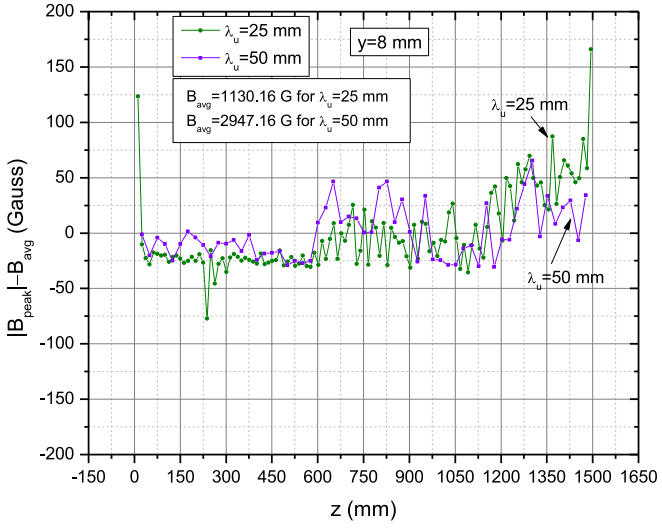

Fig. 18. Difference in peak magnetic field from the average.

another end pole design, using 1/4 and 3/4 fractional magnetic blocks ensures the integral of the magnetic field along the electron beam axis is zero. The tunability of these schemes are provided by the longitudinal displacement of the of the end magnets from the undulator ends. The scheme presented here provides an alternate method and tunability of the minimizing the field integrals. In the scheme, The 50 mm period magnet array has a conventional vertical magnetized half magnet end termination with a provision of longitudinal displacement of the end magnet while the 25 mm period magnet array has a provision of transverse displacement of the vertical magnetized end half magnet. This adds to novelty of the asymmetric magnet pole undulator. The purpose of the proposed prototype asymmetric undulator relates to the application of the pulsed wire measurement of undulator. In a pulsed wire technique, the pulse length is determined by the undulator period. In our proposed experiment, it is interesting to know the requirement of pulse length in the asymmetric undulator due to two superposed undulator periods [26,27].

CRediT authorship contribution statement

Rohit Kamle: Software, Investigation, Formal analysis. **G. Mishra:** Writing – review & editing, Writing – original draft, Project administration, Methodology, Conceptualization. **Roma Khullar:** Visualization, Supervision. **Mona Gehlot:** Supervision, Software. **Saif Mohd Khan:** Methodology.

Declaration of competing interest

The authors declare that they have no known competing financial interests or personal relationships that could have appeared to influence the work reported in this paper.

Acknowledgements

The work is supported by SERB, New Delhi, Govt. of India through a Grant No CRG/1007/2022. The authors are thankful to Dr. Manish Kumar Mehta and Mr. Kuldeep Tiwari, School of Physics, Devi Ahilya Vishwavidyalaya, Indore for their assistance in magnet array assembly.

Data availability

No data was used for the research described in the article.

References

[1] C. Yu, et al., Development of an APPLE III undulator prototype with three-dimensional force compensation for SHINE, Front. Phys. 11 (2023) 1174620, https://doi.org/10.3389/fphy.2023.1174620.
[2] T.-Y. Chung, C.-H. Chang, H. Chen, H.-H. Chen, C.-S. Hwang, From design and construction to operation of the APPLE undulator at TPS, J. Instrum. 19 (03) (2024) P03004, https://doi.org/10.1088/1748-0221/19/03/P03004.
[3] Y. Yang, et al., A new practical design of a merged APPLE-knot undulator for high energy photon source, Nucl. Instrum. Methods Phys. Res., Sect. A 1034 (2022) 166816, https://doi.org/10.1016/j.nima.2022.166816.
[4] A. Potet, et al., Bi-periodic undulator innovative insertion device for SOLEIL II, in: 14th International Particle Accelerator Conference, IPAC23, 2023, pp. 3819–3821, https://doi.org/10.18429/JACOW-IPAC2023-WEPM108. Venice.
[5] S. Zhou, W. Zhang, S. Xiang, Y. Zhu, Y. He, Y. Lei, The magnetic design of a double-period undulator based on magnetic force compensation technology, IEEE Trans. Appl. Supercond. 34 (5) (2024) 1–5, https://doi.org/10.1109/TASC.2023.3346838, 4100505.
[6] Z. Zhao, Q. Jia, Linearly and circularly polarized radiation with a low on-axis heat load from an asymmetric magnet pole undulator, Phys. Rev. Accel. Beams 25 (5) (2022) 050702, https://doi.org/10.1103/PhysRevAccelBeams.25.050702.
[7] A.B. Temnykh, Delta undulator for Cornell energy recovery linac, Phys. Rev. ST Accel. Beams 11 (12) (2008) 120702, https://doi.org/10.1103/PhysRevSTAB.11.120702.
[8] Y. Li, R. Lindberg, K.-J. Kim, Transverse gradient undulator in a storage ring x-ray free electron laser oscillator, Phys. Rev. Accel. Beams 26 (3) (2023) 030702, https://doi.org/10.1103/PhysRevAccelBeams.26.030702.
[9] M. Calvi, C. Camenzuli, E. Prat, Th. Schmidt, Transverse gradient in Apple-type undulators, J. Synchrotron Radiat. 24 (3) (2017) 600–608, https://doi.org/10.1107/S1600577517004726.
[10] E. Vescovo, et al., QP-EPU105: operational experience with a quasi-periodic undulator at NSLS II, in: Presented at the PROCEEDINGS OF THE 13TH INTERNATIONAL CONFERENCE ON SYNCHROTRON RADIATION INSTRUMENTATION – SRI2018, Taipei, Taiwan, 2019 030004, https://doi.org/10.1063/1.5084567.
[11] Ali Ramezani Moghaddam, Beni Singh, Cephise Cacho, Quasi-periodic Apple-knot undulator for Diamond Light Source, 2026, pp. 1192–1195, https://doi.org/10.18429/JACOW-IPAC2023-MOPM093.
[12] James A. Clarke, Chap. 7, in: The Science and Technology of Undulators & Wigglers, Oxford University Press, 2004.
[13] V.A. Papadichev, G.V. Rybalchenko, End field formation in planar hybrid undulators to ensure gap independence of the first and second field integrals, Nucl. Instrum. Methods Phys. Res., Sect. A 532 (3) (2004) 644–651, https://doi.org/10.1016/j.nima.2004.06.109.
[14] A. Ramezani Moghaddam, H. Ghasem, M. Lamehi Rashti, J. Rahighi, Magnetic design of the first prototype pure permanent magnet undulator for the ILSF, in: Proceedings of the 5th Int. Particle Accelerator Conf. IPAC2014, 2014, p. 387. MB, 10.18429/JACOW-IPAC2014-WEPME031.
[15] J. Chavanne, P. Elleaume, P. Van Vaerenbergh, End field structures for linear/helical insertion devices, in: Proceedings of the 1999 Particle Accelerator Conference (Cat. No.99CH36366) 4, IEEE, New York, NY, USA, 1999, pp. 2665–2667, https://doi.org/10.1109/PAC.1999.792897.
[16] Cai Genwang, Jia Qika, Design of end magnetic structures for Shanghai DUV-FEL hybrid undulators, High Power Laser and Particle Beams 17 (10) (2005) 1585–1589.

[17] A. Potet, et al., Bi-periodic undulator: Innovative insertion device for SOLEIL II, Proc. FLS2023, JACoW Publishing, Geneva, Switzerland, 2023, https://doi.org/10.18429/JACOW-FLS2023-TH1D4.
[18] Z. Wolf, "Delta undulator end design," SLAC, vol. LCLS-TN-13-2, Jan. 2013 https://www-ssrl.slac.stanford.edu/lcls/technotes/lcls-tn-13-4.pdf. (Last accessed 21-July-2025).
[19] Z. Zhao, Q. Jia, Studies on the asymmetric magnet pole undulators, Nucl. Instrum. Methods Phys. Res., Sect. A 999 (2021) 165205, https://doi.org/10.1016/j.nima.2021.165205.
[20] G. Mishra, C. Bindua, M. Gehlot, R. Khullar, Progress in development and measurement of an asymmetric magnet pole undulator, J. Phys. Conf. Ser. 2687 (8) (2024) 082032, https://doi.org/10.1088/1742-6596/2687/8/082032.
[21] J. Pflüger, G. Heintze, The asymmetric wiggler at HASYLAB, Nucl. Instrum. Methods Phys. Res., Sect. A 289 (1–2) (1990) 300–306, https://doi.org/10.1016/0168-9002(90)90273-9.
[22] J. Goulon, P. Elleaume, D. Raoux, Special multipole wiggler design producing circularly polarized synchrotron radiation, Nucl. Instrum. Methods Phys. Res., Sect. A 254 (1) (1987) 192–201, https://doi.org/10.1016/0168-9002(87)90502-X.
[23] J. Chavanne, P. Van Vaerenbergh, P. Elleaume, A 3T asymmetric permanent magnet wiggler, Nucl. Instrum. Methods Phys. Res., Sect. A 421 (1–2) (1999) 352–360, https://doi.org/10.1016/S0168-9002(98)01209-1.
[24] P. Elleaume, O. Chubar, J. Chavanne, Computing 3D magnetic fields from insertion devices, in: Proceedings of the 1997 Particle Accelerator Conference (Cat. No.97CH36167), IEEE, Vancouver, BC, Canada, 2026, pp. 3509–3511, https://doi.org/10.1109/pac.1997.753258.
[25] O. Chubar, P. Elleaume, J. Chavanne, A three-dimensional magnetostatics computer code for insertion devices, J. Synchrotron Radiat. 5 (3) (1998) 481–484, https://doi.org/10.1107/s0909049597013502.
[26] Sumit Tripathi, G. Mishra, Vinit Kumar, Sanjay Chouksey, Ravi Kumar, Pulse requirements for field integral measurements in pulsed wire method, Nucl. Instrum. Methods Phys. Res. Sect. A Accel. Spectrom. Detect. Assoc. Equip. 635 (2011) 121.
[27] Saif Mohd Khan, G. Mishra, Mona Gehlot, Pulsed wire measurement of 20 mm period hybrid undulator, WE4P38, 67th ICFA Beam Dynamics Workshop Future Light Sources, FLS-2023, Luzern, Switzerland, Sept 2023, JACOW Publishing, 2026.